

Supplementary Materials for
Engineering memory with an extrinsically disordered kinase

Cristian Ripoli *et al.*

Corresponding author: Cristian Ripoli, cristian.ripoli@unicatt.it

Sci. Adv. **9**, eadh1110 (2023)
DOI: 10.1126/sciadv.adh1110

This PDF file includes:

Figs. S1 to S9
Table S1

```

Mus musculus      MRLTLLCCTWREERMGEEGSELPCASCQRIYDGQYLQALNADWHADCFRCCECSVLSL
Rattus norveg     MRLTLLCCTWREERMGEEGSELPCASCQSIYDGQYLQALNADWHADCFRCCECSTSL
Homo Sapiens      MRLTLLCCTWREERMGEEGSELPCASCQRIYDGQYLQALNADWHADCFRCDCSASL
*****.* *****:***.***

Mus musculus      HQYYEKDQGLFCKKDYWARYGESCHGCSEHITKGLVMVAGELKYHPECFICLACGNFIGD
Rattus norveg     HQYYEKDQGLFCKKDYWARYGESCHGCSEHITKGLVMVAGELKYHPECFICLACGNFIGD
Homo Sapiens      HQYYEKDQGLFCKKDYWARYGESCHGCSEIITKGLVMVAGELKYHPECFICLTCGTFIGD
*****:*****:***.***

Mus musculus      GDTYTLVEHSKLYCGQCYYQTVVTPVIEQILPDSPGSHLPHTVTLVSI PASAHGKRGLSV
Rattus norveg     GDTYTLVEHSKLYCGQCYYQTVVTPVIEQILPDSPGSHLPHTVTLVSI PASAHGKRGLSV
Homo Sapiens      GDTYTLVEHSKLYCGHCYYQTVVTPVIEQILPDSPGSHLPHTVTLVSI PASSHGKRGLSV
*****:*****:*****

Mus musculus      SIDPPHGPPGCGTEHSHTVRVQGVDPGCMSPDVKNSIHVGDRILEINGTPIRNVPLDEID
Rattus norveg     SIDPPHGPPGCGTEHSHTVRVQGVDPGCMSPDVKNSIHIGDRILEINGTPIRNVPLDEID
Homo Sapiens      SIDPPHGPPGCGTEHSHTVRVQGVDPGCMSPDVKNSIHVGDRILEINGTPIRNVPLDEID
*****:*****

Mus musculus      LLIQETSRLQLTLEHDPHDSLGHGVPVSDPSPLSSPVHTPSGQAASSARQKPVLRSCSID
Rattus norveg     LLIQETSRLQLTLEHDPHDSLGHGVPVSDPSPLASPVHTPSGQAGSSARQKPVLRSCSID
Homo Sapiens      LLIQETSRLQLTLEHDPHDTLGHGLGPETSPLSSPAYTPSGEAGSSARQKPVLRSCSID
*****:***. . . . .***:***:***:*.*****

Mus musculus      TSPGTSSLASPASQRKDLGRSESLRVVCRPHRIFRPSDLIHGEVLGKGCFGQAIKVTHRE
Rattus norveg     TSPGAGSLVSPASQRKDLGRSESLRVVCRPHRIFRPSDLIHGEVLGKGCFGQAIKVTHRE
Homo Sapiens      RSPGAGSLGSPASQRKDLGRSESLRVVCRPHRIFRPSDLIHGEVLGKGCFGQAIKVTHRE
***:.* **********

Mus musculus      TGEVMVMKELIRFDEETQRTFLKEVKVMRCLEHPNVLKFIVGLYKDKRLNFITEYIKGGT
Rattus norveg     TGEVMVMKELIRFDEETQRTFLKEVKVMRCLEHPNVLKFIVGLYKDKRLNFITEYIKGGT
Homo Sapiens      TGEVMVMKELIRFDEETQRTFLKEVKVMRCLEHPNVLKFIVGLYKDKRLNFITEYIKGGT
*****

Mus musculus      LRGI IKNMDSQYPWSQRVSVFAKD IASGMAYLHSMNIIHRDLNSHNCLVRENRNVVVADFG
Rattus norveg     LRGI IKSMDSQYPWSQRVSVFAKD IASGMAYLHSMNIIHRDLNSHNCLVRENRNVVVADFG
Homo Sapiens      LRGI IKSMDSQYPWSQRVSVFAKD IASGMAYLHSMNIIHRDLNSHNCLVRENKVVVADFG
*****.* *****:*****

Mus musculus      LARLMI DEKNQSEDLRSLKPKDRKKRYTVVGNPYWMAPEMINGRSYDEKVDVFSFGIVLC
Rattus norveg     LARLMI DEKGQSEDLRSLKPKDRKKRYTVVGNPYWMAPEMINGRSYDEKVDVFSFGIVLC
Homo Sapiens      LARLMVDEKTQPEGLRSLKPKDRKKRYTVVGNPYWMAPEMINGRSYDEKVDVFSFGIVLC
*****:*** *.* *****

Mus musculus      EIIGRVNADPDYLPRTMDFGLNVRGFLDRYCPNPCPSFFPITVRCCDL DPEKRPSFVKL
Rattus norveg     EIIGRVNADPDYLPRTMDFGLNVRGFLDRYCPNPCPSFFPITVRCCDL DPEKRPSFVKL
Homo Sapiens      EIIGRVNADPDYLPRTMDFGLNVRGFLDRYCPNPCPSFFPITVRCCDL DPEKRPSFVKL
*****

Mus musculus      EQWLET LRMHLSGHLPLGPQLEQLERGFWET YRRGESSLPAHPEVPD
Rattus norveg     EQWLET LRMHLAGHLPLGPQLEQLERGFWET YRRGESSLPAHPEVPD
Homo Sapiens      EHWLET LRMHLAGHLPLGPQLEQLDRGFWET YRRGESGLPAHPEVPD
*:*****:*****:*****.*****

```

Fig. S1. Protein sequence alignment among mouse, rat and human forms of LIMK1. Amino acid sequence of LIMK1 is conserved among mice (NCBI Reference Sequence: NM_010717.3), rats (NCBI Reference Sequence: NM_031727.2) and humans (NCBI Reference Sequence: NM_002314.4). Insertion loop is shown in blue, E360 residue in cyan, G-loop in red and T508 residue in magenta.

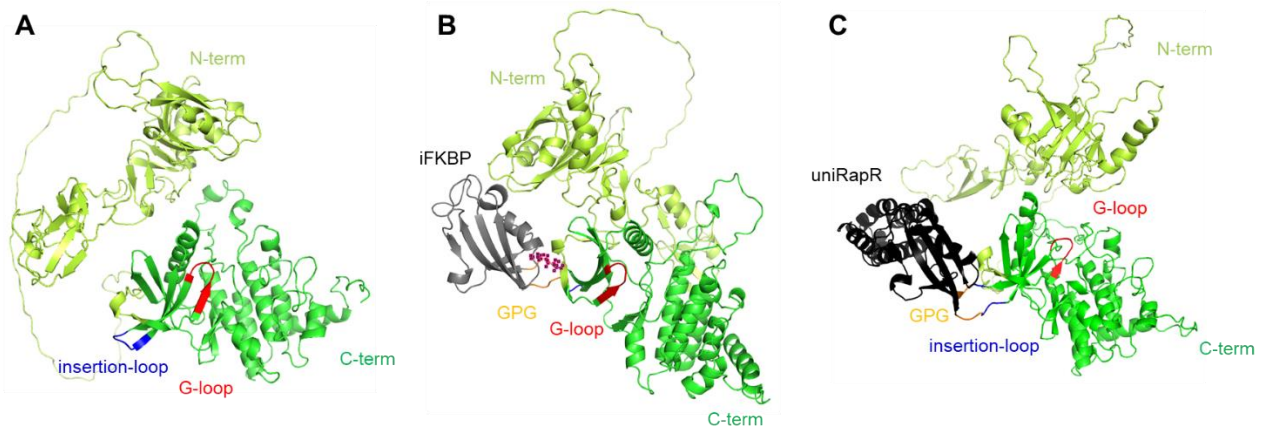


Fig. S2. Crystal structure prediction of wt and engineered LIMK1 using Alphafold2. Prediction of N- (shown in lemon) and C-term (shown in green) crystal structure of (A) LIMK1 (PDB ID: 5L6W) compared with (B) RapR-LIMK1 and (C) uniRapR-LIMK1. RapR and UniRapR in gray and black, respectively, are cloned in the insertion loop (shown in blue) - through GPG linkers (orange). The G-loop is shown in red.

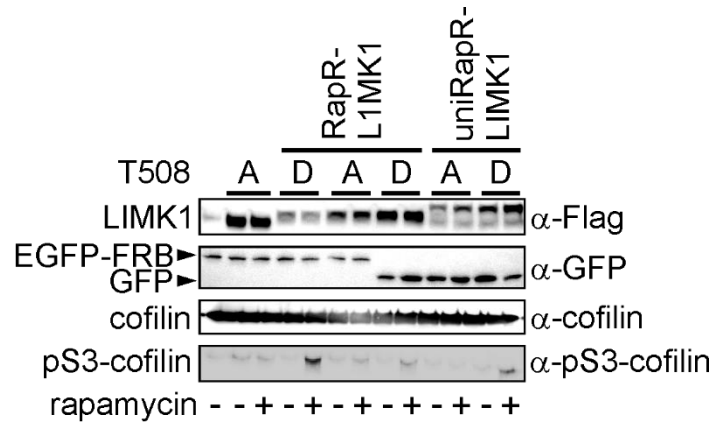


Fig. S3. Negative controls for the engineered LIMK1 analogs. The iFKBP or uniRapR domain inserted LIMK1 T508A catalytically inactive mutant or RapR-LIMK1 in the absence of FRB did not generate inducible phosphorylation of cofilin in the presence of rapamycin.

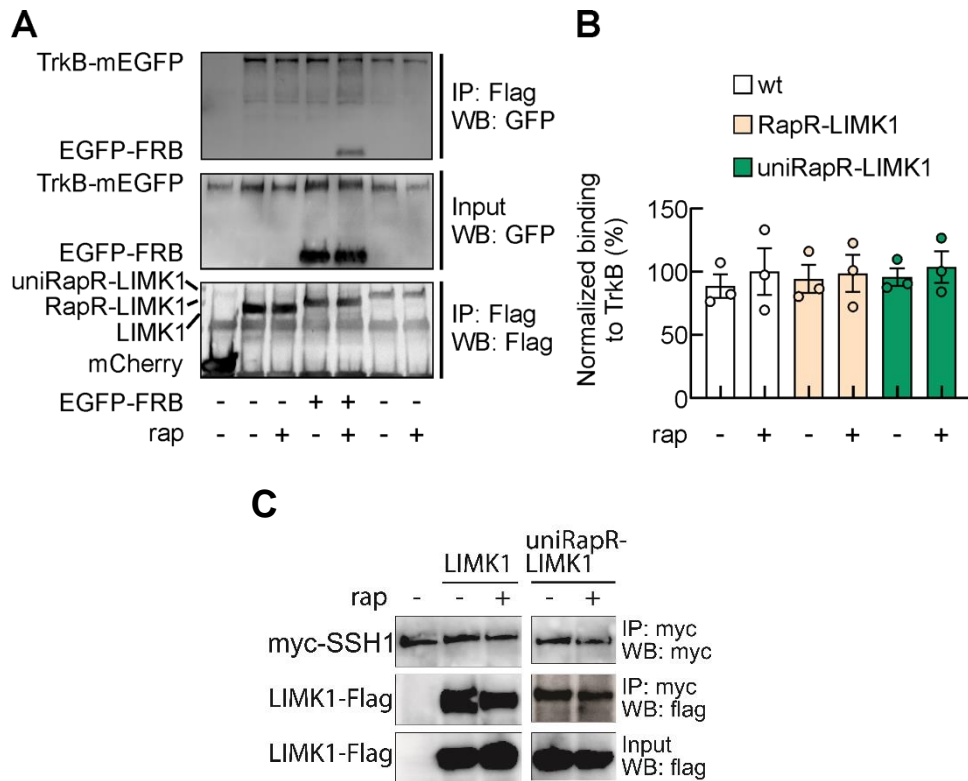


Fig. S4. LIMK1 analogs interact with TrkB and SSH1. LIMK1-Flag wt, RapR-LIMK1-Flag or uniRapR-LIMK1-Flag were co-expressed with TrkB-EGFP in HEK293T cells treated with vehicle or 200 nM of rapamycin. Cell lysates were immunoprecipitated with an anti-Flag antibody. Immunoprecipitated proteins were detected by western blot using EGFP and Flag antibodies. (A) Representative blot of LIMK1-TrkB co-immunoprecipitation. (B) The amount of immunoprecipitated (IP) TrkB signal was normalized to the total amount of TrkB (Input) signal in each condition. Data are expressed as mean \pm SEM. Statistics by one-way ANOVA with the Dunnett's post hoc test comparisons. (C) Representative blot for LIMK1-SSH1 co-immunoprecipitation. SSH tagged with Myc epitope was co-expressed in HEK293T cells with LIMK1-Flag or uniRapR-LIMK1-Flag in the presence of vehicle or 500 nM of rapamycin.

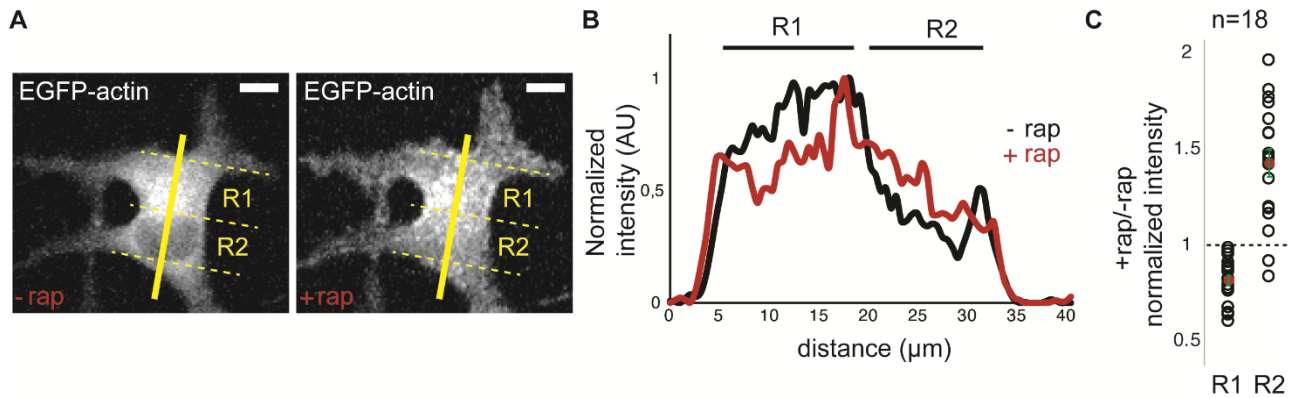


Fig. S5. Inducible actin polymerization in living cells. (A) A representative image expressing EGFP-actin before and after the addition of rapamycin. The yellow line is used for line-scan analysis. R1 region corresponds to the cytoplasmic region from the edge of the cell to the edge of the nucleus. R2 represents the nucleus. Scale bar, 10 μm . (B) The quantification of the fluorescence intensity along the line for the cell before (black) and after (red) rapamycin addition. Upon addition of rapamycin, the high-intensity cytoplasm-accumulated EGFP-actin spreads to the plasma membrane as the low-intensity nuclear signal disappears. The intensity values are normalized for each cell. (C) The ratio between each data point from the black and red curves within the R1 and R2 regions was calculated for each cell (a total of 18 cells). The ratios from each cell were shown as black circles, the mean value was shown in red sphere, and the standard error was shown in green.

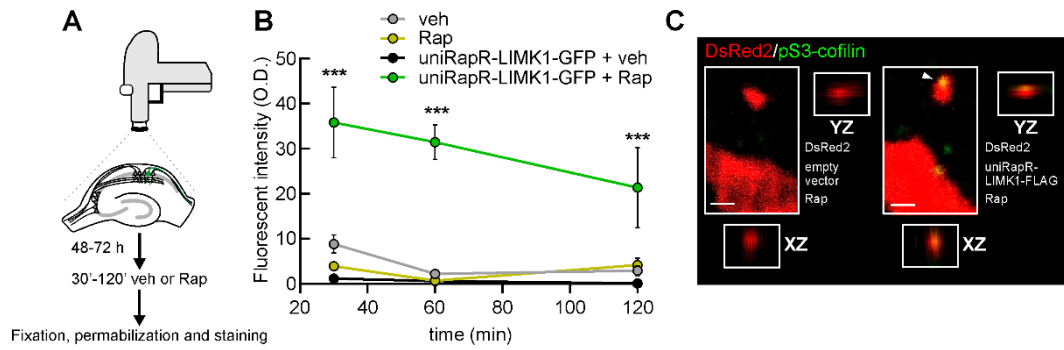


Fig. S6. Time course of pS3-cofilin during chemogenetic manipulation of LIMK1. (A) A schematic representation for the organotypic hippocampal slices transfection and treatment. (B) Quantitative analysis of the fluorescent intensity of pS3-cofilin signal in DsRed-positive neurons expressing an empty vector or uniRapR-LIMK1-Flag and treated with vehicle or rapamycin for 30, 60 and 120 min. Data are expressed as mean \pm SEM. *** $p < 0.001$. Statistics by two-way repeated-measures ANOVA with Bonferroni's post hoc test; $n = 3$ to 5 dendrites from 3 slices each condition. (C) Representative images from one experiment of DsRed2-positive neurons expressing an empty vector or uniRapR-LIMK1-Flag and treated with rapamycin for 60 min. Insets show YZ and XZ cross-sections from the Z-stack acquisitions. A representative potentiated spine is shown with a white arrow, which represents the overlap (yellow) of pS3-cofilin signal (green) and DsRed2 (red). Scale bars: 1 μ m.

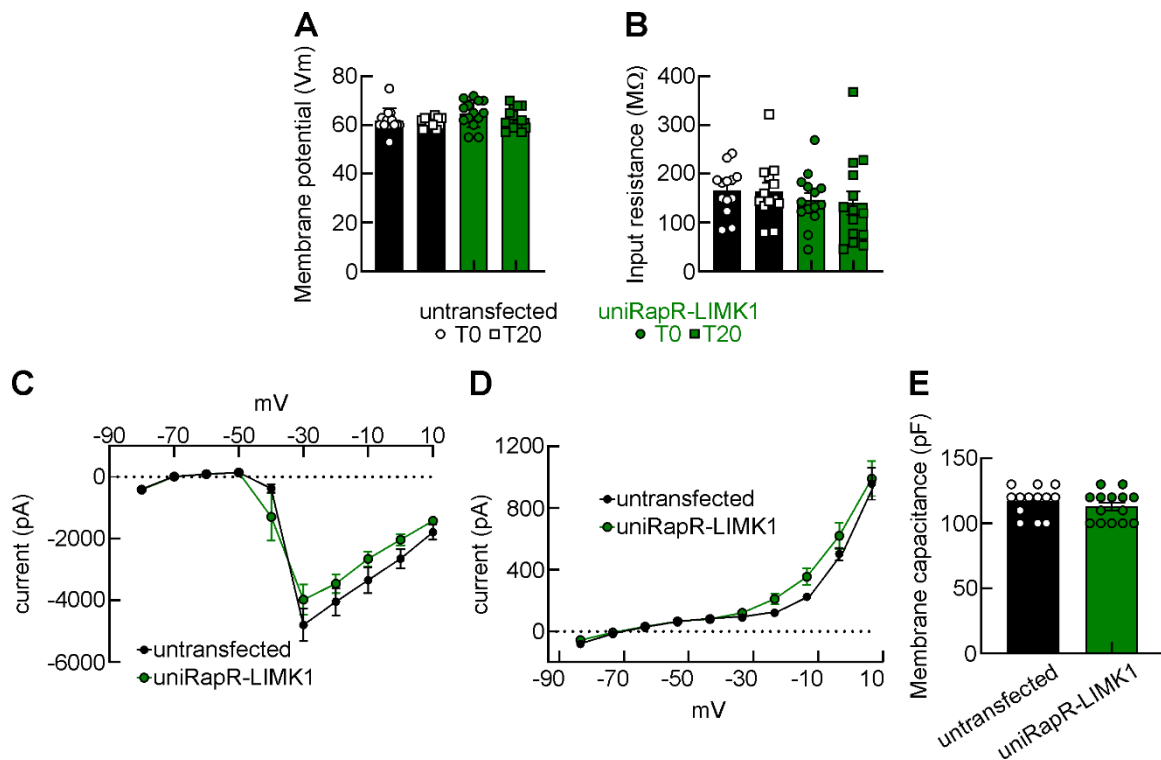


Fig. S7. UniRapR-LIMK1 expression and activation do not impact resting membrane potential, input resistance, or inward and outward voltage-dependent currents. Summary graphs of membrane potential (A) and input resistance (B) values recorded from untransfected and uniRapR-LIMK1 transfected neurons before (T0, circles) and 20 min (T20) after (squares) rapamycin application. Data are expressed as mean \pm SEM. Statistics by one-way ANOVA with the Dunnett's post hoc test comparisons. (C, D) Current-to-voltage (I-V) relationship of inward (C) and outward (D) currents recorded from untransfected and uniRapR-LIMK1 transfected neurons. Statistics by two-way repeated-measures ANOVA with Bonferroni's post hoc test comparisons. (E) Summary graphs of membrane capacitance values recorded from untransfected and uniRapR-LIMK1 transfected neurons. Data are expressed as mean \pm SEM. Statistics by two-tailed Student's *t* test.

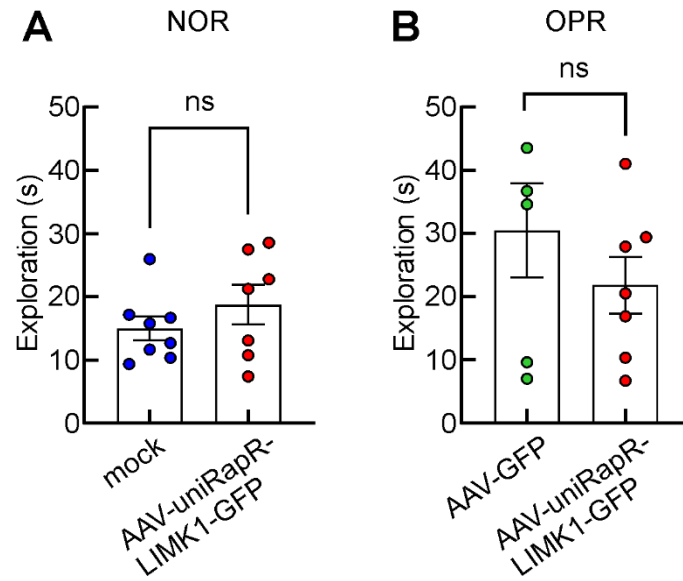


Fig. S8. Exploration time during NOR and OPR test results. Total exploration time during NOR (A) and OPR (B) tests, defined as the time during which the nose of the animal was directed towards one of the objects with a proximity of 2 cm, was similar for mock and AAV-uniRapR-LIMK1 intranasally treatment with Rap. Data are expressed as mean \pm SEM. *Ns*, not significant; Statistics by two-tailed Student's *t* test.

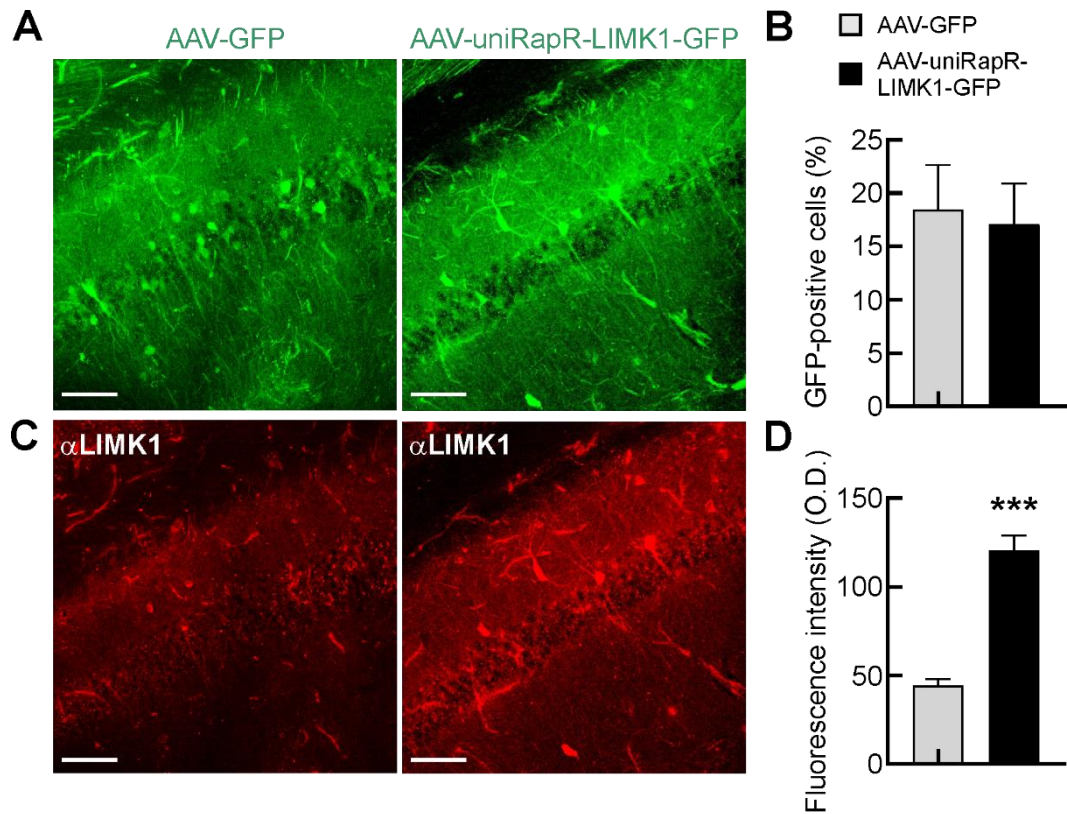


Fig. S9. Comparison of AAV infection rate and LIMK1 expression in AAV-EGFP and AAV-uniRapR-LIMK1-EGFP infected mice. Representative images showing EGFP signals (A) and immunostaining images for LIMK1 (B) within the CA1 area of the hippocampus of mice 3 weeks after systemic AAV-EGFP (left panel) and AAV-uniRapR-LIMK1-EGFP (right panel) virus injection (10-month-old). Scale bar: 100 μ m. (C) Summary graph showing the percentage of EGFP-positive cells in the hippocampi of AAV-EGFP and AAV-uniRapR-LIMK1-EGFP infected mice and (D) the fluorescence intensity signal of LIMK1 in EGFP-positive cells (n=6 sections from 3 mice each condition). Data are expressed as mean \pm SEM. ***p < 0.001; Statistics by two-tailed Student's *t* test.

Supplementary Table 1:

The volumetric increase in spine subtypes

Spine type	Volume increase (%)	n
Mushroom, M	52.08 ± 6.86	235/12
Thin, T	275.30 ± 107.60	13/12
Stubby, S	43.16 ± 12.74	65/12
Filopodia, F	48.03 ± 42.31	4/12